applied sciences

MDPI

Article

Thermogravimetric Study of Refuse Derived Fuel Produced from Municipal Solid Waste of Kazakhstan

Botagoz Kuspangaliyeva [1,2], Botakoz Suleimenova [1,2], Dhawal Shah [1] and Yerbol Sarbassov [1,2,*]

[1] Department of Chemical and Materials Engineering, School of Engineering and Digital Sciences, Nazarbayev University, Kabanbay Batyr Str., 53, Nur-Sultan 010000, Kazakhstan; botagoz.kuspangaliyeva@nu.edu.kz (B.K.); botakoz.suleimenova@nu.edu.kz (B.S.); dhawal.shah@nu.edu.kz (D.S.)

[2] Green Energy and Environment Laboratory, National Laboratory Astana, Nazarbayev University, Kabanbay Batyr Str., 53, Nur-Sultan 010000, Kazakhstan

* Correspondence: ysarbassov@nu.edu.kz; Tel.: +7-7172-70-57-52

Abstract: Efficient waste management, including proper utilization of municipal solid waste (MSW), is imperative for a sustainable future. Among several management options, pyrolysis and combustion of MSW has regained interest because of improved combustion techniques. This work aims to investigate the thermal conversion and combustion characteristics of refuse derived solid fuel (RDF) samples and its individual compounds collected from Nur-Sultan's MSW landfills. The waste-derived solid RDF samples originally consist of textile, mixed paper, and mixed plastic. In particular, the samples, including RDF and its three constituent components, were analyzed in the temperature range of 25 to 900 °C, at three different heating rates, by thermogravimetric method. The gross calorific value for RDF derived from Nur-Sultan's MSW was determined to be 23.4 MJ/kg. The weight loss rates of the samples, differential thermogravimetry (DTG), and kinetic analysis were compared between individual RDF components and for the mixed RDF. Combustion kinetics models were calculated using Flynn–Wall–Ozawa (FWO), Kissinger–Akahira–Sunose (KAS), and Friedman methods. The results revealed that first decomposition of RDF samples was observed at the range of 180–370 °C. Moreover, the activation energy for conversion of RDF was observed to be the highest among the constituent components and gradually decreased from 370 to 140 kJ/kmol.

Keywords: municipal solid waste; refuse derived fuel; thermogravimetric analysis; combustion kinetics

Citation: Kuspangaliyeva, B.; Suleimenova, B.; Shah, D.; Sarbassov, Y. Thermogravimetric Study of Refuse Derived Fuel Produced from Municipal Solid Waste of Kazakhstan. *Appl. Sci.* **2021**, *11*, 1219. https://doi.org/10.3390/app11031219

Academic Editor: Dagmar Juchelková
Received: 29 December 2020
Accepted: 21 January 2021
Published: 29 January 2021

1. Introduction

The waste management strategy of developed European Union countries employs following steps such as prevention, reuse, recycling, energy recovery and disposal [1]. Such preventive measures across EU countries have led to a significant decrease of landfilling municipal solid waste (MSW) and increase of waste recycling. An alternative to landfilling is the waste to energy (WtE) technology, which has also significantly increased with effective waste management strategies.

Considering local state, in Kazakhstan, roughly 4.3 million tons of MSW was produced in 2018, and this quantity is expected to increase to 7 M tons by 2030 [2,3]. Even though some elements of the waste management practices have been implemented in Kazakhstan, including source separation of recyclables (plastics and cardboards) and battery and electronic waste containers, the disposal of MSW in sanitary landfills is still dominates in major cities [4]. The current capital city of Kazakhstan, Nur-Sultan city (previously named as Astana city) has been growing continuously since the capital city was transferred from Almaty city in 1998 [5]. Only in the time interval of 1998–2019, the population of Nur-Sultan city has increased from 327,000 to 1,078,000 and based on this dynamics, a further increase of city's population is anticipated [5]. In 2018, around 1300 tons of MSW is generated per day in the capital city Nur-Sultan, with recycling rate of 13%. The composition of the MSW depends on the country and the applied waste management schemes, and the variations

in the MSW can be significant [6]. A detailed composition of Nur-Sultan's MSW obtained during the sampling campaigns is plotted in Figure 1.

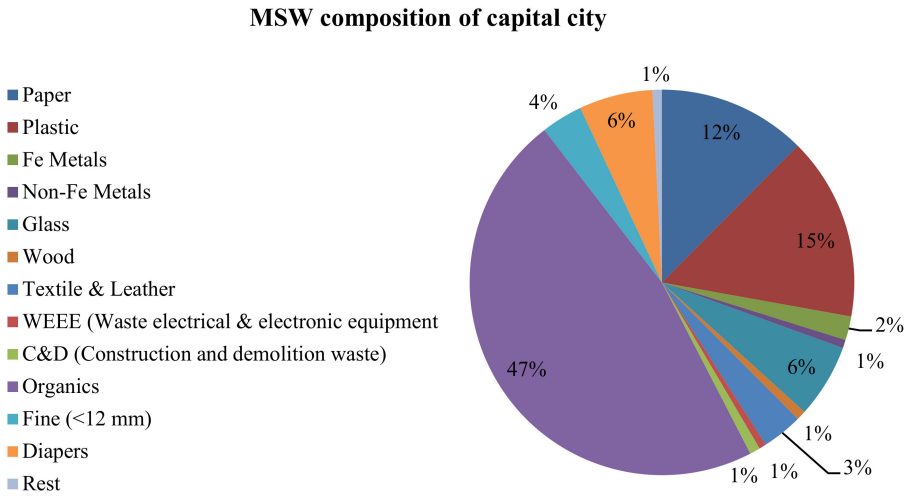

Figure 1. Average municipal solid waste (MSW) composition of Nur-Sultan city in 2018/2019.

The production of solid refuse derived fuel (RDF) from MSW can be considered as potential alternative source of fossil fuels, which can be utilized in the existing power plants [7]. RDF, as stated by Grammellis et al. [8], typically consist of mixed plastic, mixed paper, textiles, and wood fractions. Sorum et al. [9], on the other hand observed that RDF consisted of 75% of paper and 25% plastics. Comparable compounds of RDF were also reported by Cozzani et al. (1995). According to the Abylkhani et al., [10] the potential share of solid RDF in MSW of Nur-Sultan city was around 10% and has calorific values of around 20 to 23 MJ/kg. In comparison, the RDF investigated in Turkey consisted of 17% of papers, 17% of all types of plastic and remaining 66% were textile fraction [11]. Moreover, Reza et al. [12] observed that RDF composed of 26% all type of papers, 20% of plastics, 3% of textile, and 6.2% of wood/rubber or leather materials. Typical plastics in solid RDF consists of polyethylene (PE), polyethylene terephthalate (PET), polyvinyl chloride (PVC), and low and high density plastics (LDPE andHDPE, respectively) [13]. Mixed paper typically includes packaging paper, cardboard, tetra pack, newspapers, while the textile was made of general clothes.

The development of WtE technology particularly with co-firing option of solid RDF with coal in combined heat and power (CHP) plants is an optimal combustion solution [14–16]. In the cold regions, such as Kazakhstan, co-firing of solid RDF can be easily justified due to high energy demand for district heating in most cities of the country [17]. In addition, co-firing of RDF with coal also reduces the landfilling areas for MSW disposal and transportation of coal, which in turn would further mitigate greenhouse gas (GHG) emissions [18,19]. Other advantages of co-firing solid RDF and coal are that retrofitting an existing power plants (PP) does not involve high capital costs and can be flexible to switch to coal-fired when biomass or MSW supplies are unavailable [19]. Co-firing also helps to control NOx and SOx emissions [16], as low sulfur RDF tend to reduce SO_x emissions, and high moisture content of RDF decreases the flame temperature, thereby reducing NOx formation [16]. At present, the energy production of Kazakhstan is highly depended on thermal power plants, majority of which utilizes low-grade coal [17]. According to an International Energy Agency (IEA), the total CO_2 emissions from coal combustion including electricity and district heating production were 121 Mt in 2015, representing 60% of the total Kazakhstan's CO_2 emissions in recent years [20]. Therefore, efficient and sustainable development of energy generation and consumption chain is imperative, wherein WtE option can be an important contributor towards circular economy initiatives.

The co-firing of RDF with coal is an optimal solution, particularly in locations where centralized district heating system is available; however, to efficiently use RDF as fuel, it is important to determine its thermal and kinetics properties [8]. The availability of kinetic parameters is crucial to design/modify reactors for conversion of RDF [21]. Extensive studies on thermogravimetric analysis of pyrolysis and combustion of RDF had been reported in literature, including its components. A concise summary of the relevant studies is reported in Table 1. Thermogravimetric analysis tests are reliable methods of getting thermal properties of various solid fuels and temperature peaks during conversion. On the other hand, several classical kinetic methods have been developed for kinetic measurements. Such methods include first-order [22], *n*th-order reaction [23], sequential models [24], distributed activation energy model, among which, as seen from Table 1, the Flynn–Wall–Ozawa (FWO), Friedman, and the Kissinger–Akahira–Sunose (KAS) methods have been widely applied for RDF and MSW [25]. Furthermore, it can also be seen from Table 1 that kinetic reaction rates and activation energy of MSW and RDF have large variations. These variations can be attributed to the dissimilarity of RDF materials, experimental apparatus, test conditions, and analytical methods for calculation of kinetic parameters [9]. Moreover, the difference in decomposition rates between the various studies occurred mainly due to the variation of MSW compositions, which in turn depends on location, lifestyle, waste management system, and other factors of society and demography [26].

Table 1. Summary of thermochemical properties and kinetics modelling of several refuse derived solid fuel (RDF)'s/MSW's decomposition based on the literature.

Sample	Experimental Conditions				Kinetic Model	Activation Energy (kJ/mol)	Ref.
	Environment	Flow Rate (mL/min)	Temp.(°C)	Heating Rate (°C/min)			
Paper, textile (cotton), wood, plastic (PET)	N_2	60	800	10–60	Integral method	Textile: 37–56; Paper: 50–72; PET: 182–224;	[27]
Cellulosic fraction, plastics	N_2	150	500–600	10	Integral method	Cellulose: 244; Hemicellulose: 111; Lignin: 43; PS: 312; PP: 337; LDPE: 341; HDPE: 445;	[9]
Paper, wood, PE	N_2	150	500–600	20	RDF degradation rate	Cellulose: 196–217; Hemicellulose: 172/174; Lignin: 122–137; PE: 248;	[28]
Paper sludge	N_2	80	1000	30–50	FWO, KAS	MSW and paper sludge 50/50 mixture: 97 (KAS); 112 (FWO);	[29]
Paper, plastics	N_2	100	550	3–9	Classical laws of kinetics	Paper: 83–86; LDPE: 128; HDPE: 278; PS: 121; PVC: 123–299;	[30]
Paper, plastic	N_2	50	650	20	Model-fitting: 1st order reaction	Cellulose: 105–109; Hemicellulose: 141–142; Lignin: 153–154; PE: 281; PP: 236; PS: 211;	[6]
Paper, plastic	He	100	1000	20	Independent parallel, first order kinetics	Cellulose: 211; Hemicellulose: 131; Lignin: 30–48; PVC: (R1) [a] 183; (R2) 177; (R3) 378; (R4) 181;	[8]
Hemicellulose, Cellulose, Lignin, Plastics	Air	1000	1000	10–30	FWO	Cellulose: 48; Hemicellulose: 40; Lignin: 44; PS: 62; PVC: 46; PET: 76;	[13]
RDF (textile, paper, plastic, sawdust)	Air	-	800	10–30	Model-fitting: 1st order reaction	(R1) 77; (R2) 21;	[31]
MSW	Air	100	1000	20	Model-fitting: nth order reaction	(R1) 138; (R2) 80; (R3) 155;	[32]
Paper, textile, plastic	Air	30	900	10	Non-isothermal analysis method	Paper: 60–65; Textile: 51–56; Plastic: 5–92;	[33]

– [a] (R1, R2, R3, R4) are different reaction steps.

There is no literature available for the combustion characteristics of RDF samples produced in Kazakhstan. In the following wok, we discuss the thermal properties of RDF obtained from MSW of capital city of Kazakhstan over the period of 2018–2019. Both mixed and non-mixed RDF samples were decomposed in air environment and its kinetic parameters are reported herein. The effect of heating rates was discussed, and kinetics models were evaluated by Flynn–Wall–Ozawa (FWO), Kissinger–Akahira–Sunose (KAS) and Friedman methods.

2. Materials and Methods

2.1. Sample Materials

Mixed and non-mixed solid RDF fractions were collected from the MSW landfill of Nur-Sultan city during the sampling campaigns performed in 2018 and 2019. The sampling procedure was similar to those reported by Abylkhani et al. [10]. During the first step sorting, recyclables and organics are separated, followed by second step sorting. RDF samples in this work were taken from the second step sorting and consisted of mixed paper 37.8%, mixed plastic 53.3%, textile 8.9%, and traces of wood, Figure 2. Considering its insignificant amount in the MSW, wood was eliminated from this study [10]. The collected fraction of mixed paper, plastic, and textile fractions were further treated in garden shredder and in a knife mill for size reduction, to obtain homogenized fine powders

with particle sizes between 200 and 400 µm. Treated RDF samples that were used for TGA tests are shown in Figure 3. Further, all samples were sterilized in the autoclave at temperature of 121 °C and dried at 105 °C for 24 h [34].

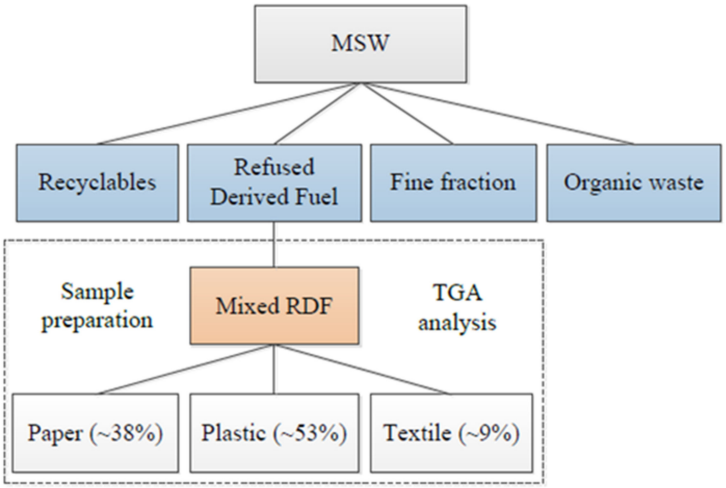

Figure 2. Procedure for sampling of RDF and its constituent components.

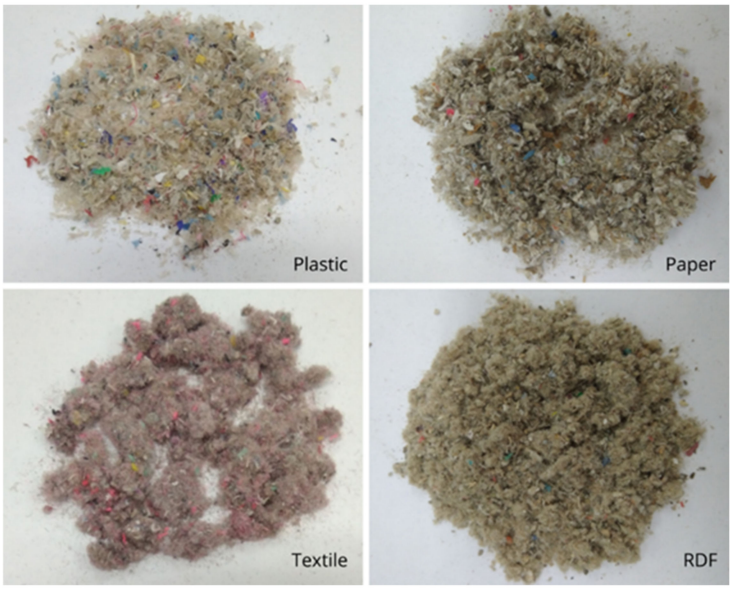

Figure 3. RDF and its fractions before the experiment.

Proximate analysis of samples was carried out according to the ASTM standard (D1762-84). Elemental CHNS analyzer (Vario Micro Cube, Elementar) was used for the ultimate analysis. The proximate and ultimate analysis of the RDF and its fractions are presented in Table 2. Thermal properties of RDF were roughly comparable with those noted in the literature (Grammelis et al. [8], Efika et al. [35], Fan et al. [36] and Zhou et al. [37]). The calorific values of the samples were determined by a bomb calorimeter with weights of samples ranging between 0.3 and 1.0 g.

Table 2. Proximate analysis, ultimate analysis, and calorific values of the samples.

Proximate (wt%, as Received)	RDF	Plastic	Paper	Textile
Moisture	1.5	0.8	2.6	1.2
Volatile matter	86.7	87.3	85.7	86.7
Ash	8.2	8.7	8.5	4.0
Fixed carbon	3.6	3.2	3.2	8.1
Ultimate (wt%, and dry ash free)				
Carbon	66.5	83.5	46.8	47.8
Hydrogen	9.9	13.0	6.4	6.1
Nitrogen	0.6	0.5	0.6	1.3
Sulfur	0.2	0.3	0.1	0.2
Oxygen *	22.8	2.7	46.1	44.6
Gross Calorific value (MJ/kg) **	23.4	32.6	16.4	20.1

* by difference; ** measured by bomb calorimeter.

2.2. Apparatus and Procedure

The decomposition of RDF and its fractions as mixed paper, mixed plastic, and textile samples were conducted in a TGA-DSC analyzer (Perkin Elmer STA 6000). The samples were thermally treated from ambient to a set temperature of 900 °C in an air environment with the air flow rate of 20 mL/min. Furthermore, effect of heating rates on decomposition of RDF was performed by varying the heating rates at 10, 20 and 30 °C/min. The weight of samples was in the range of 4–10 mg. For the reproducibility of results, all experiments were performed in duplicate.

2.3. Kinetics of RDF Samples

Due to the heterogeneous phases and complexity of the reaction steps in RDF samples, combustion characteristics of RDF and its fractions, isoconversional kinetics analysis were conducted. The rate of equation for solid phase reactions for heterogeneous RDF could be expressed as Equation (1):

$$\frac{d\alpha}{dt} = k(t)f(\alpha) = Aexp\left(-\frac{E}{RT}\right)(1-a) \quad (1)$$

where $\frac{d\alpha}{dt}$ is the rate of conversion, $k(t)$ is the rate of constant, $f(\alpha)$ is depends on the reaction model, A is the pre-exponential Arrhenius factor (s^{-1}), E is the apparent activation energy (kJ/mol), R is the universal gas constant, and T is the reaction temperature (K). The conversion rate (α) was defined from the following Equation (2):

$$\alpha = \frac{m_o - m_t}{m_o - m_f} \quad (2)$$

where m_o is the initial weight of the sample; m_t is the weight at time t, and m_f is the final weight of the samples. Reaction kinetics was applied to the thermal data determined under non-isothermal conditions with a constant heating rate. For non-isothermal measurements linear heating rate, β is defined as β = dT/dt, thus Equations (1) and (2) could be given as [29,38,39]:

$$\frac{d\alpha}{dT} = \left(\frac{A}{\beta}\right)\exp\left(-\frac{E_a}{RT}\right)f(\alpha) \quad (3)$$

Two different approaches were found as most commonly used models for integral isoconventional (free model) methods, which are FWO [25] and Kissinger–Akahira–Sunose (KAS) methods [22]. FWO method assumes the change in the apparent activation energy is constant during the thermal process and uses Doyle's approximation [40,41]. Thus,

rearranging and integrating both sides of Equation (3) and with the Doyle's approximation, Equation (3) can be modified as [13,38]:

$$log\beta = \log\left(\frac{AE_a}{Rg(\alpha)}\right) - 2.315 - 0.4567\frac{E}{RT} \quad (4)$$

where the integration function $g(\alpha)$ is considered as a constant value for a given conversion α and it does not affect the activation energy. The activation energy E can be determined by the linear relationship between $log\beta$ and 1/T at different heating rates but same conversion.

The expression of KAS method applies approximation of $p(u) = x^{-2}e^{-u}$ to Equation (4). After rearranging, the expression becomes as [38]:

$$ln\left(\frac{\beta}{T_\alpha^2}\right) = \ln\left[\frac{AR}{E_a g(\alpha)}\right] - \frac{E}{RT} \quad (5)$$

As in the previous method, the activation energy E can be obtained by the slope of straight line $ln\left(\frac{\beta}{T^2}\right)$ vs. 1/T and R is 8.314 J/mol K.

In addition to these kinetic models, Friedman method is assumed as isoconversional differential method which is expressed as below [42]:

$$ln\left(\frac{d\alpha}{dt}\right) = \ln[f(\alpha)A_\alpha] - \frac{E}{RT} \quad (6)$$

Conversional function $f(\alpha)$ in Friedman method is constant. It describes reaction, which is independent from the temperature and depends on mass loss rate. The activation energy was calculated by using the slope of $\ln\left(\frac{d\alpha}{dt}\right)$ vs. 1/T plot.

3. Results and Discussions

3.1. Thermogravimetry (TG) and Differential Thermogravimetry (DTG) Curves of RDF Samples

The weight loss curves (TG curve) of RDF and its compounds at 10 °C/min were shown in Figure 4. As seen from the figure, the initial weight loss of samples occurred at the temperature of 100 °C, which can be attributed to the release of moisture. The moisture release for samples were in the following order, plastic (0.4–1.5%) < textile (1.5–2.0%) < paper (4.0–4.5%) and for the RDF varied in the 2.0–2.5% range. In the temperature range of 370 and 400 °C, the weight loss was greater for the paper samples, followed by mixed RDF, plastic and textile fractions. In addition, more than 80% of samples were decomposed when the temperature reached 500 °C (see Figure 4). However, when the temperature exceeded 550 °C, the weight loss of textile was higher in comparison to the plastic, paper, and mixed RDF. Furthermore, minor weight losses were observed for all samples at temperatures more than 600 °C and these losses can be attributed to the end of conversion stage. The residual weight for plastic and paper samples were roughly 8–10% and only around 4.3% for textile. Similar low residual weight of cotton samples were also observed by Font [43] through their TGA analysis.

In the temperature range of 200 and 600 °C, three main decomposition peaks were observed for textile and mixed RDF samples, while this was different for mixed plastic and mixed paper samples. Such differences in the DTG curves for plastic can be explained by the presence of several types of plastic materials, which may lead to several peaks [8,13]. The first decomposition interval of samples takes place between 180 °C and 370 °C, with peaks being at 330 °C. Similar temperature range for RDF decomposition were observed by Skodras et al. [44], Grammelis et al. [8], and Çepelioğullar et al. [38]. As also noted by Skodras et al. [44], the decomposition of RDF samples at these temperature range mainly occurs due to the release of volatiles, followed by the gas phase reactions between the volatiles and oxygen. Mixed paper and plastic, on the other hand, shows the highest and lowest decomposition rate in the first peak, respectively (Figure 4). According to Miskolczi

et.al [6], Su et.al [45], the first peak represents mostly the degradation of hemicellulose and cellulose, while the second peak attributes to the degradation of plastics such as PE and PP.

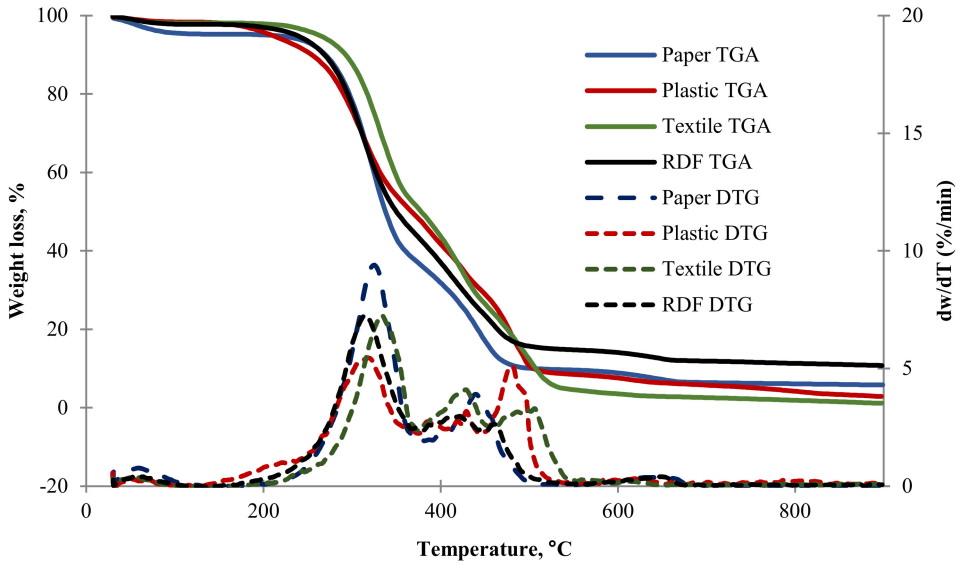

Figure 4. Weight loss curves (TG) and weight loss rates (DTG) of samples at 10 °C/min.

In other studies, the paper and plastic samples had only one peak, except PVC which produced two peaks [8,13]. Grammelis et al. [8] have reported that the total conversion of several plastic samples were practically 100%, except for PVC which accounted for 91.7%. A higher residual mass in plastic, that we observed in our experiments, could be due to the presence of PVC in the mixed plastic. Several DTG peaks between 400 and 600 °C in plastic samples clearly indicates the presence of different types of plastics. It is also worth noting herein that the mixed paper can contain impurities, including tetra pack. It is well known that tetra pack is made of wood-based material coated with PE and aluminum. The DTG curve for mixed paper in Figure 4 shows two peaks that correspond to degradation of cellulose followed by decomposition of plastic based materials, respectively.

3.2. Effect of Heating Rate

Effect of heating rates on the combustion behavior of paper, plastic, textile, and RDF mixture was presented with three different heating rates of 10, 20, and 30 °C/min (see Figure 5a–d, respectively). The results reveal that the weight loss curves of RDF samples were delayed and shifted towards high temperatures with an increase of the heating rates from 10 to 30 °C/min. These results with delay of weight loss curves and shift of weight loss rate to a higher temperatures were consistent with studies of Luo et al. [13] and Font et al., [43]. In addition, the effect of heating rate was more significant for the temperature between 250 and 550 °C, for all the samples. Although, in comparison to the weight loss curves of paper (Figure 5a), plastic (Figure 5b), and textiles (Figure 5c), the effect of heating rate on RDF samples (Figure 5d) were not so significant, which can be explained by the presence of mixture of components in the RDF.

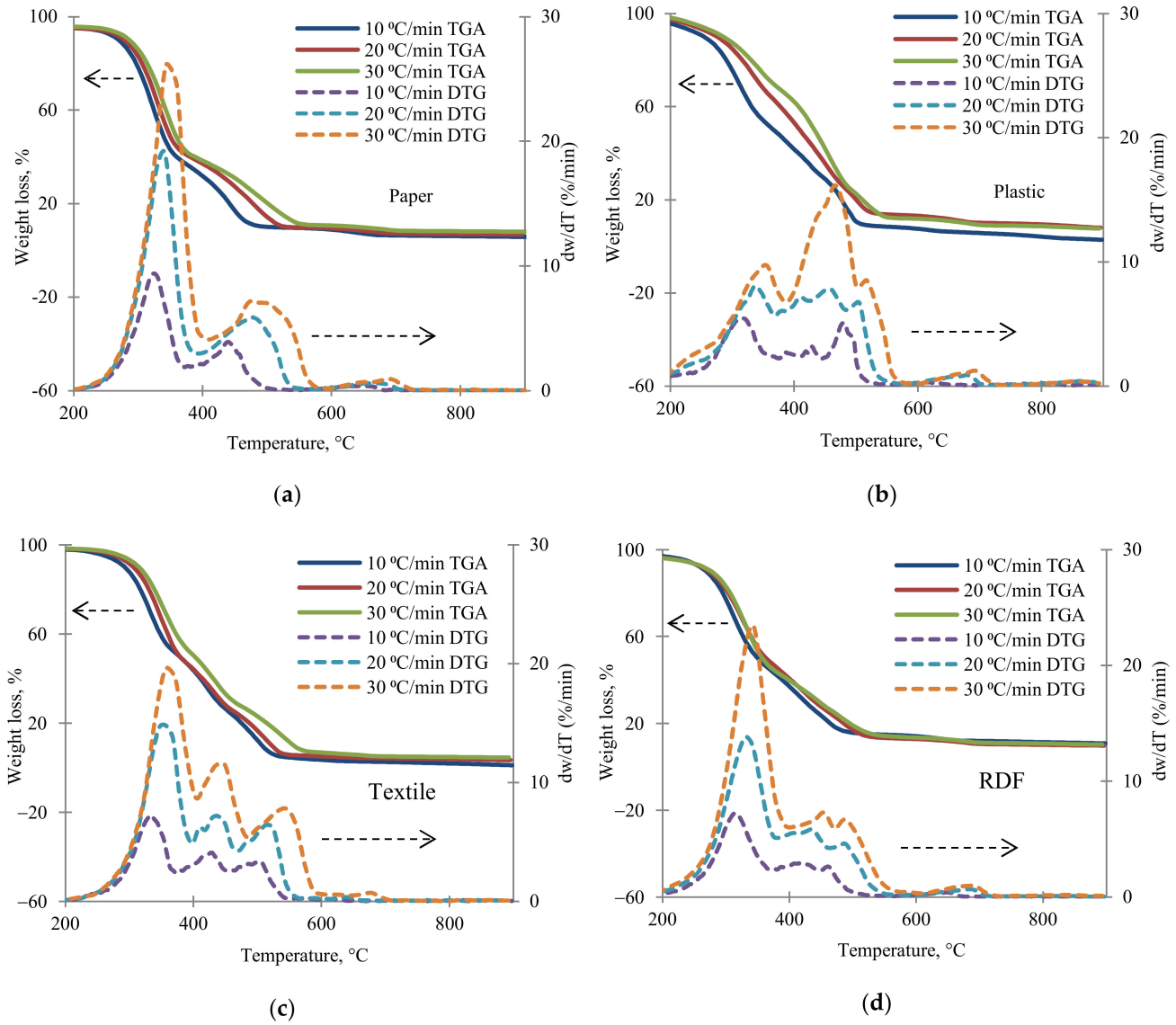

Figure 5. Effect of heating rate on TG/DTG curves of (**a**) mixed paper, (**b**) plastic, (**c**) textile, (**d**) RDF.

Table 3 presents the DTG peaks and peak characteristics for all the four samples under study at different heating rates. Three major peaks were observed for paper during all three heating rates, namely, at 320–329 °C, 434–471 °C, and 640–679 °C (Figure 5a). The difference of first DTG peaks was 10%/min between the tests with heating rates of 10 to 20 °C/min. Then this difference was decreased to 6%/min when heating rate was further increased to 20 to 30 °C/min. This delay of weight loss at the higher heating rates is due to the high decomposition rate of paper within the temperature range of 320 to 329 °C. Figure 5b shows that there are five weight loss peaks in the DTG profile in 10 °C/min and 20 °C/min, while in 30 °C/min, there are only four weight loss peaks. This may result from the reaction overlap occurring in the range of 400–450 °C or it could also be due to the mixed content of plastic. The maximum weight loss rate increases from 9.4%/min to 26.1%/min for paper, from 5.5%/min to 9.7%/min for plastic, from 7.3%/min to 19.7%/min for textile and from 7.3%/min to 23.3%/min for RDF, when the heating rate varied from 10 °C/min to 30 °C/min, as is shown in Table 3. We also note that the increase of the heating rate results in higher weight residuals, but some inconsistencies do occur due to the heterogeneous content of sample. In general, the heating rate could affect the samples combustion. Furthermore, since the mass of samples were less than 20 mg for

TGA experiment, the shapes and uneven distribution of MSW might affect and deviate the results [46].

Table 3. Differential thermogravimetry (DTG) peak characteristics of paper, plastic, textile, and RDF samples during combustion.

Sample	Paper			Plastic			Textile			RDF		
Heating rate (°C/min)	10	20	30	10	20	30	10	20	30	10	20	30
DTG_1 (%/min)	9.4	19.9	26.1	5.5	8.1	9.7	7.3	14.8	19.7	7.3	13.8	23.3
Temperature at DTG_1 (°C)	320	329	326	312	326	340	328	347	344	309	319	326
DTG_2 (%/min)	3.9	5.5	7.1	3.2	7.8	16.2	4.1	7.2	11.4	3.0	5.8	7.3
Temperature DTG_2 (°C)	434	458	471	424	450	451	424	429	434	417	426	440
DTG_3 (%/min)	0.4	0.5	0.9	5.1	6.7	8.5	3.3	6.4	7.8	2.6	4.6	6.7
Temperature at DTG_3 (°C)	640	662	679	476	495	500	502	504	531	457	478	471
DTG_4 (%/min)	-	-	-	0.3	0.9	1.2	0.2	0.4	0.7	0.4	0.7	1.0
Temperature at DTG_4 (°C)	-	-	-	614	671	678	607	631	663	645	672	663

3.3. Combustion Kinetics

Linear plots by FWO, KAS, and Friedman methods for RDF samples were prepared and shown in Supplementary Figure S1a–c. The plots showed good correlations and were used to calculate activation energy at each conversion rate (<0.9). The correlation coefficients of these methods were all above 0.9 for RDF (except $\alpha = 0.6$), which suggests that these methods are applicable for defining the activation energy based on the TGA data. The results of an activation energy calculated for RDF are shown in Table 4. Since FWO, KAS and Friedman models produced almost similar results, we used FWO method for analysis of the components of RDF (mixed paper, mixed plastic, and textile). A similar procedure was used for the other samples, and the linear plots and kinetic parameters provided in the Supplementary Materials part as Figures S2–S4 and Tables S1–S3, respectively. The relationship between the calculated activation energy and conversion rate for all samples is shown in Figure 6.

Figure S1 shows the isoconversional lines of FWO, KAS, and Friedman methods. It can be seen that FWO and KAS plots have good correlation. The activation energy values from Friedman methods are slightly lower than other methods, as noted in Table 4. The activation energy was recorded as 365.27, 375.13, and 331.47 kJ/mol at $\alpha = 0.1$ for each model. The slight increase in the activation energy was found at $\alpha = 0.7$ in all three methods, which means that there was the energy requirement for the final decomposition step of RDF.

Table 4. Kinetic parameters of RDF fraction by Flynn–Wall–Ozawa (FWO), Kissinger–Akahira–Sunose (KAS), and Friedman methods.

α	FWO			KAS			Friedman		
	A (min^{-1})	E_a (kJ/mol)	R^2	A (min^{-1})	E_a (kJ/mol)	R^2	A (min^{-1})	E_a (kJ/mol)	R^2
0.1	1.10×10^{35}	365.27	1.00	4.88×10^{35}	375.13	1.00	7.47×10^{29}	331.47	1.00
0.2	1.55×10^{21}	236.04	0.98	2.55×10^{21}	238.74	0.98	7.58×10^{17}	215.22	0.99
0.3	1.71×10^{18}	208.55	0.94	2.06×10^{18}	209.57	0.94	2.41×10^{15}	191.04	0.95
0.4	8.90×10^{16}	197.52	0.87	9.17×10^{16}	197.74	0.85	2.47×10^{14}	182.18	0.87
0.5	2.66×10^{16}	195.28	0.69	2.54×10^{16}	195.11	0.66	1.46×10^{14}	182.41	0.68
0.6	7.94×10^{8}	111.15	0.27	2.14×10^{8}	106.17	0.23	1.61×10^{7}	102.72	0.25
0.7	4.78×10^{15}	203.62	0.81	4.06×10^{15}	202.83	0.80	6.84×10^{13}	193.26	0.81
0.8	2.69×10^{12}	169.23	0.67	1.40×10^{12}	166.09	0.96	6.57×10^{10}	159.3	0.97
0.9	7.52×10^{9}	140.31	0.98	2.37×10^{9}	135.00	0.97	3.69×10^{8}	131.11	0.98
Mean	1.22×10^{34}	203		5.42×10^{34}	202.93		8.30×10^{28}	187.63	
SD	3.67×10^{34}	71.63		1.63×10^{35}	76.16		2.49×10^{29}	63.99	

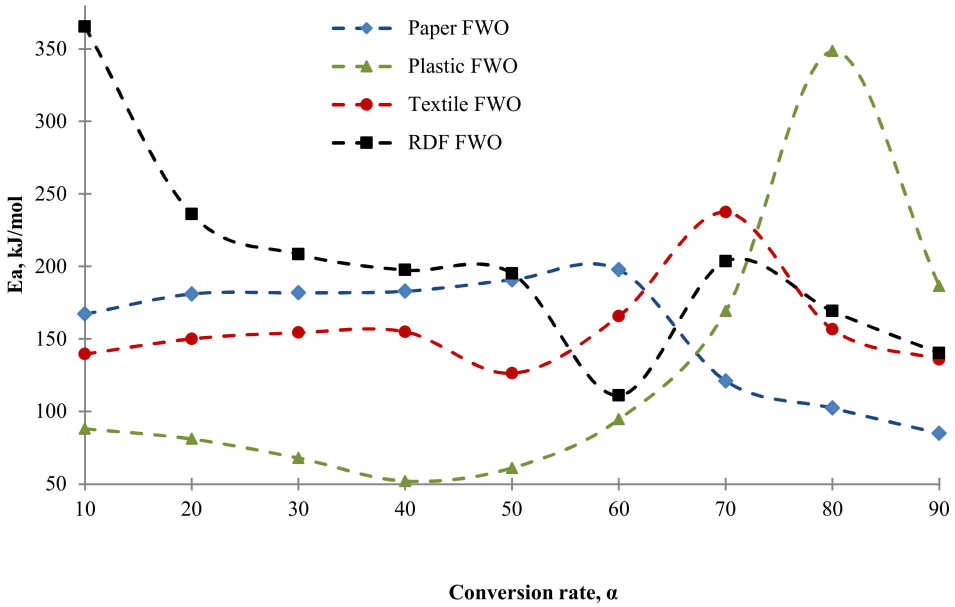

Figure 6. The relationship between activation energy and conversion rate.

It is important to notice that the correlation coefficients significantly decreased for textile and RDF fractions during combustion. There are three combustion regimes that could occur, namely diffusion-controlled, intermediate, and kinetically controlled regimes. The results, as observed from Figure S1a–c reveals that at low temperatures, 292–370 °C for textile and 264–319 °C for RDF, kinetically controlled combustion occurred. As the temperature increases to 375 °C for textile and 320 °C for RDF, the combustion regime changed to intra-particle diffusion regime, which led to a decline of correlation coefficients. Kinetic parameters of RDF samples calculated by FWO, KAS, and Friedman methods shown in Table 4. It can be noted that the regression coefficient (R^2) of RDF samples have shown higher values in most points of conversion, except one point of 0.6 (see Table 4).

Lastly, as shown in Figure 6, the activation energies of RDF and its fractions, viz., paper, textile, and plastic varied significantly as conversion rate were changed. The activation energies of paper increased slightly and then decreased at higher conversion rates. This is consistent with the literature and is due to gradual degradation of cellulose that finally results in ash. In case of textile, fluctuations were observed in the activation energies, which occurred due to textile content. The reason of first increase in the activation energy can be due to decomposition of aliphatic polyester while the second increase can be due to decomposition of aromatic polyester, which is used in the textile production. Interestingly, the higher activation energies were not required for plastic combustion at lower conversion rate. However, there was a peak at 348 kJ/ mol, which can be a sign of dechlorination or the hydrocarbon decomposition. The curve of E_a vs. α for RDF samples gradually decreased from ~370 to ~140 kJ/kmol. With conversion rate up to $\alpha < 50$, the relationships were slightly above the other compounds, while $\alpha > 50$ onward, the relationship was found between the curves of plastics, paper and textile. Overall, the relationship of E_a vs. α of RDF samples were still closer to other compounds as shown in Figure 6.

4. Conclusions

The thermogravimetric characteristics and kinetic behavior of plastic, paper, textile, and RDF were examined at three different heating rates. The results reveal that the measured calorific values of RDF derived from Nur-Sultan's MSW were similar to those noted in the literature. This suggests that with proper strategy of waste management and its implementation, a considerable amount of RDF (10 to 15% of total MSW) can be

utilized for energy production in Kazakhstan. We also observed that with an increase of heating rate, the weight loss rates of RDF and other samples increase and the reaction moves towards high temperature. Moreover, the peaks in the DTG curves indicate the presence of different types of plastics in the plastic samples, different textiles in the textile samples, and multiple components in RDF samples. Lastly, the average activation energy of the RDF was observed to be higher than that of other samples. In summary, Nur-Sultan's MSW thermogravimetric properties are reported and in near future, further work to be conducted on the lab-scale fluidized bed unit to explore its combustion efficiencies.

Supplementary Materials: The following are available online at https://www.mdpi.com/2076-3417/11/3/1219/s1, Figure S1: (a) Linear plots of logβ vs. 1/T by using FWO method for RDF; (b) Linear plots of ln(β/T^2) vs. 1/T by using KAS method for RDF; (c) Linear plots of ln(dα/dt) vs. 1/T by using Friedman method for RDF. Figure S2: Linear plots of logβ vs. 1/T by using FWO method for plastic; Figure S3: Linear plots of logβ vs. 1/T by using FWO method for textile; Figure S4: Linear plots of logβ vs. 1/T by using FWO method for paper; Table S1: Kinetic parameters of plastic fraction by FWO; Table S2: Kinetic parameters of textile fraction by FWO; Table S3: Kinetic parameters for paper by FWO.

Author Contributions: All the authors contributed equally to conducting and writing this paper. All authors have read and agreed to the published version of the manuscript.

Funding: This research was funded by the Nazarbayev University (NU), Grant number SOE2019011: "Co-firing of coal and biomass under air and oxy-fuel environments in fluidized bed rig: Experiments with process model development" and project N 3-2020/003-2020 entitled: "Development of MSW combustion and incineration technology for Astana (Kazakhstan) and investigation of MSW blending effects on reactivity of coals in CFB combustion and gasification process" and the APC was funded by SOE2019011.

Institutional Review Board Statement: Not applicable.

Informed Consent Statement: Not applicable.

Data Availability Statement: Not applicable.

Acknowledgments: Authors would like to acknowledge Berik Aimbetov for his support on the experimental part and participation in the sampling campaigns.

Conflicts of Interest: The authors declare no conflict of interest.

References

1. European Parliament and Council. Directive 2008/98/EC of the European Parliament and of the Council of 19 November 2008 on waste and repealing certain directives Waste framework. *Off. J. Eur. Union* **2008**, *312*, 3–30.
2. Government of Kazakhstan. *Programma-Modernizacii-Tbo*; Government of Kazakhstan: Nur-Sultan, Kazakhstan, 2020.
3. KazNIIEK. *Guidelines for the Calculation of Greenhouse Gas Emissions in the Atmosphere from Municipal SolidWaste Landfills*; KazNIIEK: Almaty, Kazakhstan, 2010.
4. Sarbassov, Y.; Sagalova, T.; Tursunov, O.; Venetis, C. Survey on household solid waste sorting at source in developing economies: A case study of nur-sultan city in Kazakhstan. *Sustainability* **2019**, *11*, 6496. [CrossRef]
5. *Technical Assistance Report (Project Number: 51353-001): Astana Integrated Water Master Plan Republic of Kazakhstan*; Asian Development Bank: Nur-Sultan, Kazakhstan, May 2018.
6. Miskolczi, N.; Buyong, F.; Williams, P.T. Thermogravimetric analysis and pyrolysis kinetic study of Malaysian refuse derived fuels. *J. Energy Inst.* **2010**, *83*, 125–132. [CrossRef]
7. Garg, A.; Smith, R.; Hill, D.; Simms, N.; Pollard, S. Wastes as co-fuels: The policy framework for solid recovered fuel (SRF) in Europe, with UK implications. *Environ. Sci. Technol.* **2007**, *41*, 4868–4874. [CrossRef] [PubMed]
8. Grammelis, P.; Basinas, P.; Malliopoulou, A.; Sakellaropoulos, G. Pyrolysis kinetics and combustion characteristics of waste recovered fuels. *Fuel* **2009**, *88*, 195–205. [CrossRef]
9. Sorum, L.; Gronli, M.G.; Hustad, J.E. Pyrolysis characteristics and kinetics of municipal solid wastes. *Fuel* **2001**, *80*, 1217–1227. [CrossRef]
10. Abylkhani, B.; Aiymbetov, B.; Yagofarova, A.; Tokmurzin, D.; Venetis, C.; Poulopoulos, S.; Sarbassov, Y.; Inglezakis, V.J. Seasonal characterisation of municipal solid waste from Astana city, Kazakhstan: Composition and thermal properties of combustible fraction. *Waste Manag. Res.* **2019**, *37*, 1271–1281. [CrossRef] [PubMed]

11. Kara, M. Environmental and economic advantages associated with the use of RDF in cement kilns. *Resour. Conserv. Recycl.* **2012**, *68*, 21–28. [CrossRef]
12. Reza, B.; Soltani, A.; Ruparathna, R.; Sadiq, R.; Hewage, K. Environmental and economic aspects of production and utilization of RDF as alternative fuel in cement plants: A case study of Metro Vancouver Waste Management. *Resour. Conserv. Recycl.* **2013**, *81*, 105–114. [CrossRef]
13. Luo, J.; Li, Q.; Meng, A.; Long, Y.; Zhang, Y. Combustion characteristics of typical model components in solid waste on a macro-TGA. *J. Therm. Anal. Calorim.* **2018**, *132*, 553–562. [CrossRef]
14. Piao, G.; Aono, S.; Yamazaki, R.; Mori, S.; Fujima, Y.; Kondoh, M.; Yamaguchi, M. Combustion Test of Refuse Derived Fuel in Fluidized Bed. *Waste Manag.* **2000**, *20*, 443–447. [CrossRef]
15. Rudra, S.; Tesfagaber, Y.K. Future district heating plant integrated with municipal solid waste (MSW) gasification for hydrogen production. *Energy* **2019**, *180*, 881–892. [CrossRef]
16. Genon, G.; Brizio, E. Perspectives and limits for cement kilns as a destination for RDF. *Waste Manag.* **2008**, *28*, 2375–2385. [CrossRef] [PubMed]
17. Sarbassov, Y.; Kerimray, A.; Tokmurzin, D.; Tosato, G.C.; De Miglio, R. Electricity and heating system in Kazakhstan: Exploring energy efficiency improvement paths. *Energy Policy* **2013**, *60*, 431–444. [CrossRef]
18. Haykiri-Acma, H.; Kurt, G.; Yaman, S. Properties of Biochars Obtained from RDF by Carbonization: Influences of Devolatilization Severity. *Waste Biomass Valoriz.* **2017**, *8*, 539–547. [CrossRef]
19. Roni, M.S.; Chowdhury, S.; Mamun, S.; Marufuzzaman, M.; Lein, W.; Johnson, S. Biomass co-firing technology with policies, challenges, and opportunities: A global review. *Renew. Sustain. Energy Rev.* **2017**, *78*, 1089–1101. [CrossRef]
20. IEA. *CO2 Emissions from Fuel Combustion 2017*; OECD Publishing: Paris, France, 2017; Available online: https://www.iea.org/subscribe-to-data-services/co2-emissions-statistics (accessed on 27 January 2021).
21. Cho, J.; Chu, S.; Dauenhauer, P.J.; Huber, G.W. Green Chemistry Kinetics and reaction chemistry for slow pyrolysis of enzymatic hydrolysis lignin and organosolv extracted lignin derived from maplewood. *Green Chem.* **2012**, *14*, 428–439. [CrossRef]
22. Kissinger, H.E. Variation of Peak Temperature with heating rate in differential thermal analysis. *J. Res. Natl. Bur. Stand.* **1956**, *57*, 217–221. [CrossRef]
23. Kissinger, H.E. Reaction kinetics in differential thermal analysis. *Anal. Chem.* **1957**, *303*, 1702–1706. [CrossRef]
24. Braun, R.L.; Burnham, A.K. Analysis of chemical reaction kinetics using a distribution of activation energies and simpler models. *Energy Fuels* **1987**, *1*, 153–161. [CrossRef]
25. Flynn, J.H.; Wall, L.A. A quick, direct method for the determination of activation energy from thermogravimetric data. *Polym. Lett.* **1966**, *4*, 323–328. [CrossRef]
26. Muthuraman, M.; Namioka, T.; Yoshikawa, K. A comparative study on co-combustion performance of municipal solid waste and Indonesian coal with high ash Indian coal: A thermogravimetric analysis. *Fuel Process. Technol.* **2010**, *91*, 550–558. [CrossRef]
27. Ansah, E.; Wang, L.; Shahbazi, A. Thermogravimetric and calorimetric characteristics during co-pyrolysis of municipal solid waste components. *Waste Manag.* **2016**, *56*, 196–206. [CrossRef] [PubMed]
28. Cozanni, V.; Petarca, L.; Tognotti, L. Devolatilization and pyrolysis of refuse derived fuels: Characterization and kinetic modelling by a thermogravimetric and calorimetric approach. *Fuel* **1995**, *74*, 903–912. [CrossRef]
29. Fang, S.; Yu, Z.; Lin, Y.; Hu, S.; Liao, Y.; Ma, X. Thermogravimetric analysis of the co-pyrolysis of paper sludge and municipal solid waste. *Energy Convers. Manag.* **2015**, *101*, 626–631. [CrossRef]
30. Lin, K.; Wang, H.P.; Liu, S.; Chang, N. Pyrolysis kinetics of refuse-derived fuel. *Fuel Process. Technol.* **1999**, 103–110. [CrossRef]
31. Li, Y.; Wang, H.; Li, R.; Chi, Y. Thermogravimetric analysis on the combustion characteristics of refuse-derived fuel under an oxygen-enriched atmosphere. *Biofuels* **2015**, *7269*, 217–222. [CrossRef]
32. Lai, Z.; Ma, X.; Tang, Y.; Lin, H. A study on municipal solid waste (MSW) combustion in N_2/O_2 and CO_2/O_2 atmosphere from the perspective of TGA. *Energy* **2011**, *36*, 819–824. [CrossRef]
33. Guo, X.; Wang, Z.; Li, H.; Huang, H.; Wu, C.; Chen, Y. A Study on Combustion Characteristics and Kinetic Model of Municipal Solid Wastes. *Energy Fuels* **2001**, *15*, 1441–1446. [CrossRef]
34. Robinson, T.; Bronson, B.; Gogolek, P.; Mehrani, P. Sample preparation for thermo-gravimetric determination and thermo-gravimetric characterization of refuse derived fuel. *Waste Manag.* **2016**, *48*, 265–274. [CrossRef]
35. Efika, E.C.; Onwudili, J.A.; Williams, P.T. Products from the high temperature pyrolysis of RDF at slow and rapid heating rates. *J. Anal. Appl. Pyrolysis* **2015**, *112*, 14–22. [CrossRef]
36. Fan, Y.; Yu, Z.; Fang, S.; Lin, Y.; Lin, Y.; Liao, Y.; Ma, X. Investigation on the co-combustion of oil shale and municipal solid waste by using thermogravimetric analysis. *Energy Convers. Manag.* **2016**, *117*, 367–374. [CrossRef]
37. Zhou, H.; Long, Y.; Meng, A.; Li, Q.; Zhang, Y. Classification of municipal solid waste components for thermal conversion in waste-to-energy research. *Fuel* **2015**, *145*, 151–157. [CrossRef]
38. Çepelioğullar, Ö.; Haykiri-Açma, H.; Yaman, S. Kinetic modelling of RDF pyrolysis: Model-fitting and model-free approaches. *Waste Manag.* **2016**, *48*, 275–284. [CrossRef] [PubMed]
39. Burnham, A.K. Computational aspects of kinetic analysis. Part D: The ICTAC kinetics project—multi-thermal–history model-fitting methods and their relation to isoconversional methods. *Thermochim. Acta* **2000**, *355*, 165–170. [CrossRef]
40. Doyle, C.D.; Figure, F. Kinetic Analysis of Thermogravimetric Data. *J. Appl. Polym. Sci.* **1961**, *5*, 285–292. [CrossRef]
41. Doyle, C.D. Estimating isothermal life from thermogravimetric data. *J. Appl. Polym. Sci.* **1962**, *6*, 639–642. [CrossRef]

42. Friedman, H.L. Kinetics of thermal degradation of char-forming plastics from thermogravimetry. Application to a phenolic plastic. *J. Polym. Sci. Part C Polym. Symp.* **2007**, *6*, 183–195. [CrossRef]
43. Font, R.; Conesa, J.A.; Martı, I.; Molto, J. Thermogravimetric analysis during the decomposition of cotton fabrics in an inert and air environment. *J. Anal. Appl. Pyrolysis* **2006**, *76*, 124–131. [CrossRef]
44. Skodras, G.; Grammelis, P.; Basinas, P.; Prokopidou, M.; Kakaras, E.; Sakellaropoulos, G.P. A thermochemical conversion study on the combustion of residue-derived fuels. *Water Air Soil Pollut. Focus* **2009**, *9*, 151–157. [CrossRef]
45. Su, G.; Yang, J.; Lu, H. Experimental Study on Combustion Characteristics of Three Biomass Components. *Adv. Mater. Res.* **2014**, *954*, 309–312. [CrossRef]
46. Zhou, H.; Meng, A.; Long, Y.; Li, Q.; Zhang, Y. Classification and comparison of municipal solid waste based on thermochemical characteristics. *J. Air Waste Manag. Assoc.* **2014**, *64*, 597–616. [CrossRef] [PubMed]